Reaction of the Coordinatively Unsaturated Methylene Complex $Ir{=}CH_2[N(SiMe_2CH_2PPh_2)_2]$ with Olefins: Stereoselective Formation of Allyl Hydride Derivatives

Michael D. Fryzuk,* Xiaoliang Gao, and Steven J. Rettig†

Contribution from the Department of Chemistry, University of British Columbia, 2036 Main Mall, Vancouver, BC, Canada V6T 1Z1

Received July 26, 1994⊗

Abstract: The reactivity of the coordinatively unsaturated methylene complex $Ir{=}CH_2[N(SiMe_2CH_2PPh_2)_2]$ with olefins is described. In all cases, carbon−carbon bond formation is observed with the isolation of Ir(III) allyl hydride derivatives $Ir(\eta^3\text{-}C_3H_4R)H[N(SiMe_2CH_2PPh_2)_2]$ (R = H, CN, Ph, and CO_2Me). With ethylene, exo and endo allyl hydride isomers are formed; with acrylonitrile, anti-exo and syn-endo diastereomers result and with both styrene and methyl acrylate, only the corresponding syn-endo derivative is isolated. The reaction is facilitated by electron-withdrawing olefins since propene, ethyl vinyl ether and norbornene fail to react with the methylene complex. Variable-temperature NMR studies have provided some information on the mechanism of the reaction; it is suggested that the olefin approaches the iridium−methylene complex to generate a perpendicular binding of the olefin which then undergoes C−C bond formation via migratory insertion to generate a highly puckered iridacyclobutane. Rapid β-elimination results in the formation of an isomeric allyl hydride species (detected by NMR spectroscopy) that isomerizes to the observed final products. Molecular orbital calculations (INDO-1 using CAChe Worksystem) support the idea that the olefin binds to the metal perpendicular to the π-system of the iridium−carbon double bond. Suggestions are made regarding the observed dependence on the nature of the metal center to direct the reaction to form allyl hydride derivatives or undergo olefin metathesis. $Ir(\eta^3\text{-}C_3H_4CN)H[N(SiMe_2CH_2PPh_2)_2]$, **2b**, crystallizes as a (1:1) toluene solvate, monoclinic, a = 10.884(1) Å, b = 18.672(2) Å, c = 20.169(3) Å, β = 100.32(2)°, Z = 4, space group $P2_1/c$; and crystals of $Ir(\eta^3\text{-}C_3H_4Me)H[N(SiMe_2CH_2PPh_2)_2]$, **3e**, are also monoclinic, a = 13.606(2) Å, b = 14.687(4) Å, c = 17.672(3) Å, β = 100.86(1)°, Z = 4, space group $P2_1/n$. The structures were solved by Patterson methods and were refined by full-matrix least-squares procedures to R = 0.032 and 0.034 (R_w = 0.028 and 0.033) for 6304 and 4226 reflections with $I \geq 3\sigma(I)$, respectively.

Introduction

Attempts to understand how metal complexes mediate the formation of carbon−carbon bonds is a central theme in organometallic chemical research.[1] A much studied example is the reaction of metal−carbon double bonds, such as those found in metal complexes of carbenes and alkylidenes, with olefins, which leads to different products, depending on the particular metal and its associated ancillary ligands.[2−5] Scheme 1 outlines this process in detail. The common intermediate appears to be a metallacyclobutane, and from this point olefin metathesis (path **a**), cyclopropanation (path **b**), or β-elimination to ultimately homologate an olefin (path **c**) are possible reaction pathways. Studies on the reactivity of metallacyclobutanes, prepared by ring opening reactions of cyclopropanes or halide displacements by diGrignards,[6] have shown that paths **b** and **c** are viable; however, as yet there has been no clear demonstration of the connection of a metal−carbene complex to an allyl hydride intermediate via its reaction with an olefin except by inference.[7−10] Indeed, the overwhelming reactivity patterns of

Scheme 1

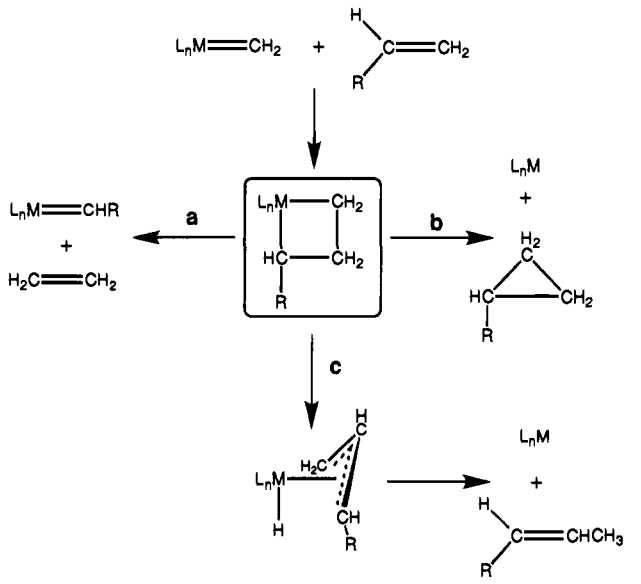

† Professional Officer: UBC Departmental X-ray Service.

⊗ Abstract published in *Advance ACS Abstracts,* February 15, 1995.

(1) Collman, J. P.; Hegedus, L. S.; Norton, J. R.; Finke, R. G. *Principles and Applications of Organotransition Metal Chemistry*; University Science Books: Mill Valley, 1987; pp 459−486.

(2) Schubert, U. *Advances in Metal Carbene Chemistry*; Kluwer Academic: Dordrecht, 1989; Vol. 279.

(3) (a) Doyle, M. P. *Chem. Rev.* **1986**, *86*, 919. (b) Casey, C. P.; Polichnowski, S. W.; Shusterman, A. J.; Jones, C. R. *J. Am. Chem. Soc.* **1979**, *101*, 7282.

(4) Feldman, J.; Schrock, R. R. *Prog. Inorg. Chem.* **1991**, *39*, 1.

(5) Dragutan, V.; Balaban, A. T.; Dimonie, M. *Olefin Metathesis and Ring Opening Polymerization of Cycloolefins*; Wiley: Bucharest, 1985.

(6) Puddephatt, R. J. *Coord. Chem. Rev.* **1980**, *33*, 149.

(7) Thorn, D. L. *Organometallics* **1982**, *1*, 879.

(8) Roper, W. R. In *Advances in Metal Carbene Chemistry*; Schubert, U., Ed.; Kluwer Academic: Dordrecht, 1989; Vol. 269, p 27.

(9) McLain, S. J.; Wood, C. D.; Schrock, R. R. *J. Am. Chem. Soc.* **1977**, *99*, 3519.

(10) Wolf, J.; Brandt, L.; Fries, A.; Werner, H. *Angew. Chem., Int. Ed. Engl.* **1990**, *29*, 510.

0002-7863/95/1517-3106$09.00/0

metal−carbene complexes with olefins are either metathesis via path **a** or cyclopropanation via path **b** or modifications thereof.[3,5]

Sometime ago, we reported[11] the preparation of the iridium(I) methylene complex **1**, and recently we detailed an improved synthesis and outlined some of its reactivity patterns.[12] This

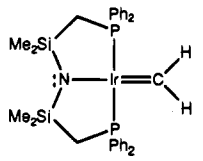

1

complex is rather unique since it is the only methylene complex of iridium that is both thermally stable and has been structurally characterized.[7,8,13−16] More importantly, of all the methylene derivatives known, **1** is the only one that has 16 valence electrons and therefore is coordinatively unsaturated. We have already shown that this coordinative unsaturation at the metal center facilitates a number of further transformations via oxidative addition and ligand coordination.[12,17] In this paper we report the reactivity of the methylene complex with olefins to produce allyl hydride derivatives. What becomes apparent from this work is that there are exacting requirements for the electronic and steric properties of the olefins. Moreover, the stereoselectivity of the reaction is particularly noteworthy and has implications in the mechanism of the formation of putative iridacyclobutane intermediates.

Results and Discussion

General Aspects. Not all olefins react with the methylene complex **1**. Only those olefins that can be considered to be electron deficient were found undergo carbon−carbon bond formation to generate the allyl hydride complexes **2** and **3** (eq 1). Although each example will be discussed in turn, the

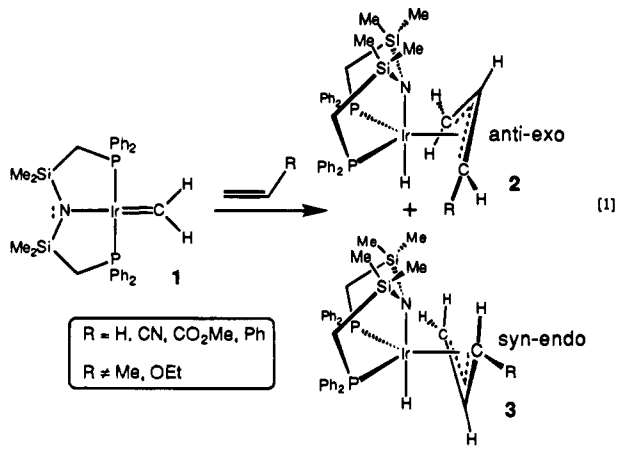

[1]

following simple olefins were found to result in allyl hydride products: ethylene (R = H); acrylonitrile (R = CN), methyl acrylate (R = CO_2Me), and styrene (R = Ph). The only disubstituted olefin that reacted cleanly with **1** was methacrylontrile (H_2C=C(Me)CN). Certain olefins were completely unreactive to the methylene complex **1** even after being heated for 12 h at 80 °C; for example, norbornene, propene (R = CH_3), and ethyl vinyl ether (R = OEt) were found to be inert with **1** and only starting materials were recovered after the reaction. Some other olefins were found to react with the methylene complex as evidenced by the discharge of the deep purple color of **1**; however, no clean products could be isolated or identified. Examples of olefins exhibiting this behavior are vinyl chloride (R = Cl) and dimethyl fumarate (*trans*-$MeO_2C(H)C$=$C(H)CO_2Me$). The stereochemistry of the observed products depends very much on the nature of the substituent; in addition, the rates of the reaction depend on both the size of the substituent and its electron-withdrawing capability.

With regard to the products, the designations syn and anti refer to the allyl moiety only and follow the standard practice of indicating the relationship of a substituent R at the terminus to the central proton. The endo and exo descriptors, however, are typical of this class of complexes and refer to the diastereomers that result from the mode of attachment of the allyl unit to the metal complex in relation to the tridentate ligand: when the central proton of the allyl points toward the amide donor of the ancillary ligand, the exo designation is used (i.e., complex **2** in eq 1), and when the central proton points toward the hydride ligand, the endo descriptor is used (i.e., complex **3** in eq 1).

Reaction with Ethylene. The reaction of the iridium methylene complex **1** with ethylene is rather slow. Addition of 10−20 equiv of C_2H_4 to **1** results in the formation of two isomeric allyl hydride complexes **2a** and **3a** along with a third complex, the square-planar iridium(I) ethylene derivative Ir(η^2-C_2H_4)[N($SiMe_2CH_2PPh_2$)$_2$] (**4**) as outlined in eq 2. At room

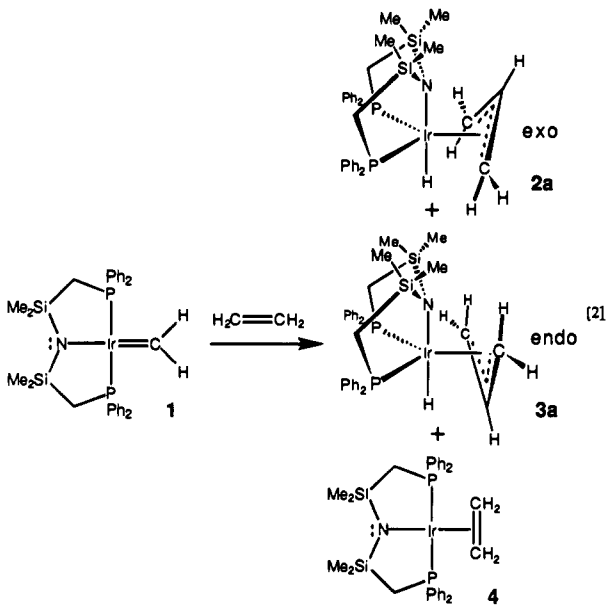

[2]

temperature, the reaction required 40 h to go to completion with a 10-fold excess of ethylene. The characterization of both **2a** and **3a** was accomplished mainly by solution NMR spectroscopy. The $^{31}P\{^1H\}$ NMR spectrum of the stereoisomers **2a** and **3a** was not particularly revealing since only singlets are observed for each species. However, in the ^1H NMR spectrum, each complex gives rise to distinct peaks; the hydride resonance of each diastereomer appears as triplet (coupling due to cis phosphine donors) upfield at approximately −20 ppm and the allyl proton peaks are diagnostic of C_s symmetry (each allyl moiety displays two equivalent syn and two equivalent anti protons). Assignment of syn and anti protons was made on

(11) Fryzuk, M. D.; MacNeil, P. A.; Rettig, S. J. *J. Am. Chem. Soc.* **1985**, *107*, 6708.
(12) Fryzuk, M. D.; Gao, X.; Joshi, K.; MacNeil, P. A.; Massey, R. L. *J. Am. Chem. Soc.* **1993**, *115*, 10581.
(13) Mango, F. D.; Dvoretzky, I. *J. Am. Chem. Soc.* **1966**, *88*, 1654.
(14) Clark, G. R.; Roper, W. R.; Wright, A. H. *J. Organomet. Chem.* **1984**, *273*, C17.
(15) Thorn, D. L.; Tulip, T. H. *J. Am. Chem. Soc.* **1981**, *103*, 5984.
(16) Klein, D. P.; Bergman, R. G. *J. Am. Chem. Soc.* **1989**, *111*, 3079.
(17) Fryzuk, M. D.; Joshi, K.; Chadha, R. J.; Rettig, S. J. *J. Am. Chem. Soc.* **1991**, *113*, 8724.

the basis of NOE difference experiments as outlined in the Experimental Section. This kind of experiment was also found to be invaluable in distinguishing the exo isomer from endo form since irradiation of the hydride resonance of the endo isomer **3a** resulted in enhancement of the central proton (H_1) of the allyl moiety by 15%; a similar experiment on the exo isomer **2a** showed no enhancement of the central proton, but a 13% enhancement of the anti protons of the allyl fragment was measured.

Monitoring this reaction as a function of time provided some insight into the reaction mechanism. The addition of 10 equiv of C_2H_4 to methylene **1** in C_6D_6 at room temperature (sealed NMR tube) results in a color change after 30 min from deep purple to brownish orange; spectroscopically, the only species observable are methylene **1** and the ethylene complex **4**, in the approximate ratio of 70:30, respectively. At this point, **4** has almost reached its maximum concentration, and now **1** begins to slowly decrease in concentration concomitant with the formation of two intermediates, the ethylene adduct of **1**, $Ir{=}CH_2(\eta^2\text{-}C_2H_4)[N(SiMe_2CH_2PPh_2)_2]$ (**5a**), and the allyl hydride complex **6a** which is isomeric to the final products **2a** and **3a**.

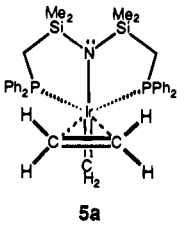

5a

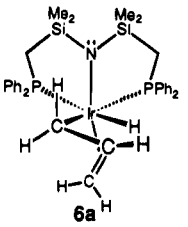

6a

The ethylene adduct **5a** was characterized by a shift in the methylene resonance ($Ir{=}CH_2$) from 16.3 to 12.5 ppm (triplet, $^3J_{PH}$ = 9.5 Hz) in the ^1H NMR spectrum; when the ^{13}C-labeled methylene complex $Ir{=}^{13}CH_2[N(SiMe_2CH_2PPh_2)_2]$ was used, a doublet of triplets was observed due to the additional carbon-13 coupling constant $^1J_{CH}$ = 144 Hz. In addition, the $^{31}P\{^1H\}$ NMR spectrum showed a singlet at 8.44 ppm. Although other isomeric stereochemistries for **5a** are possible, this particular geometry with the tridentate ligand facial and the methylene unit trans to the amide best matches other intermediates and the stereochemistry of the final product (see below).

The hydride intermediate **6a** was characterized by a doublet of doublets at −14.4 ppm with one large coupling constant ($^2J_{PH}$ = 154.1 Hz) typical of a hydride trans to phosphorus and a smaller coupling ($^2J_{PH}$ = 26.0 Hz) due to a cis-disposed phosphorus-31 nucleus; the inequivalent phosphines in **6a** are confirmed by the $^{31}P\{^1H\}$ NMR spectrum which shows two broad doublets at 8.31 and −10.88 ppm ($^2J_{PP}$ = 10.5 Hz). Only a stereochemistry having the tridentate ligand facial as shown for **6a** is consistent with these spectral data.

At the same time that the intermediates **5a** and **6a** are observed, there is still some starting methylene complex present, at least in the initial stages, the product allyl hydride derivatives **2a** and **3a** are growing in, and the ethylene complex **4** is observed; at the end of the reaction, **4** accounts for about 40% of the iridium-containing products. While all of these derivatives can be identified fairly easily by $^{31}P\{^1H\}$ NMR spectroscopy, the ^1H NMR spectra as a function of time show complicated overlapping multiplets, particularly in the region of 1−5 ppm where the allyl protons typically resonate; as a result, assignment of the proton resonances of the coordinated ethylene of **5a** and the allyl protons of **6a** was not possible.

The isomeric product allyl hydride complexes **2a** and **3a** do not grow in at the same rate. In separate experiments where the methylene complex was allowed to react with a large excess of ethylene (>50 equiv), thereby reducing the time of the reaction, the exo allyl hydride complex **2a** was the first of the final products formed; further monitoring of the reaction showed that the exo isomer slowly isomerizes to the endo isomer **3a** to ultimately produce an approximately 1:1 mixture of these two diastereoisomers.

The reaction of the deuterated methylene complex **1**-d_2, $Ir{=}CD_2[N(SiMe_2CH_2PPh_2)_2]$, with ethylene gives analogous results to that described above. For the intermediate **5a**, the resonance of the methylene ligand is not observed; the allyl hydride intermediate **6a** does show a hydride resonance. The ^1H NMR spectra of the final allyl hydride products are consistent with the methylene unit ending up at one of the termini of the allyl groups; this is evident from integration since the resonances due to the central proton of the allyl ligand, $H_{central}$, integrate accurately as one proton as do the hydride resonances, whereas the syn and anti protons, H_{syn} and H_{anti}, respectively, also integrate as one proton, each corresponding to half the value for the undeuterated material. The ethylene adduct **4** in this reaction is formed completely undeuterated (eq 3).

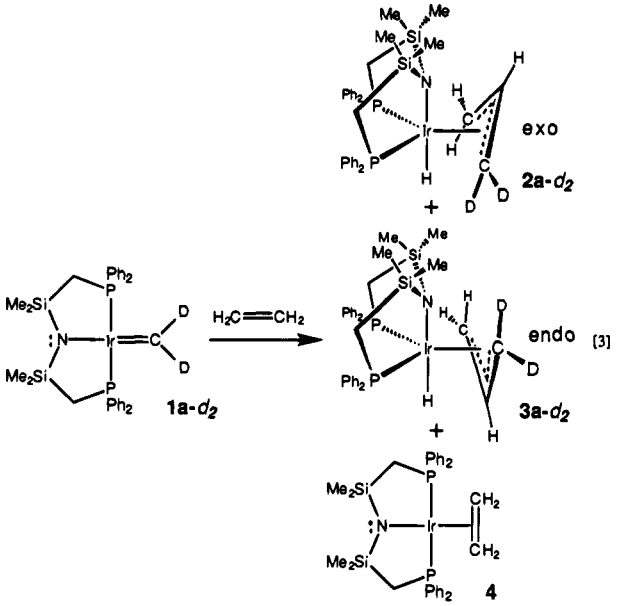

1a-d_2 **2a**-d_2 **3a**-d_2 **4** [3]

As already mentioned, the complexity of the ^1H NMR spectrum of this mixture of intermediates and products did not allow assignment of endo versus exo of the intermediate hydride **6a** by NOE difference experiments.

Two questions still remain to be answered: (i) how does the ethylene complex **4** form? and (ii) what is the fate of the methylene unit in **1** in the formation of **4**? The complexity of the ^1H NMR spectrum of this mixture of iridium complexes, particularly in the region of 1−5 ppm did not provide any clues as to the fate of the methylene unit. So, to answer these points, the ^{13}C-labeled methylene complex $Ir{=}^{13}CH_2[N(SiMe_2CH_2PPh_2)_2]$ was allowed to react with excess ethylene under conditions comparable to those of the above reactions. Analysis of the crude reaction mixture by $^{13}C\{^1H\}$ NMR spectroscopy showed the formation of the exo (**2a**) and endo (**3a**) allyl complexes as a doublet of doublets at 32.1 ppm (J_{PC} = 28.43 Hz, J_{PC} = 2.22 Hz) and 45.0 ppm (J_{PC} = 31.70 Hz, J_{PC} = 2.88 Hz), respectively, due to the terminal carbons of the allyl moiety. At the end of the reaction there was one other peak at 30.14 ppm that could not be accounted for in terms of iridium-containing products.

The crude reaction mixture was further analyzed by being filtered through basic alumina and then subjecting the filtrate

to GC–MS; the results showed that there was formation of a series of homologous hydrocarbons of the formula C_nH_{2n} (n = 8–35). Attempts to detect smaller hydrocarbons (n < 8) were not successful due to solvent interference. These hydrocarbons are proposed to be 1-olefins since the GC retention times matched those of authentic terminal olefins determined by spiking the crude reaction mixture. The $^{13}C\{^1H\}$ NMR spectrum of the filtered reaction mixture of olefinic hydrocarbons, prepared from $Ir{=}^{13}CH_2[N(SiMe_2CH_2PPh_2)_2]$ and unlabeled ethylene, showed only a single peak at 30.1 ppm; the complementary reaction of ^{13}C-labeled ethylene, $H_2{}^{13}C{=}{}^{13}CH_2$, and unlabeled methylene **1** showed a number of singlets in the region 24–30 ppm in the $^{13}C\{^1H\}$ NMR spectrum. The 30.1 ppm peak corresponds to the labeled methylene unit near the middle of the oligomer. Our best estimates of mass balance are that the olefinic homologous series of hydrocarbons accounts for 30 ± 10% of the original starting methylene **1** and therefore corresponds to the formation of the ethylene complex **4**. However, separate experiments have shown that these olefinic hydrocarbons are not produced when excess ethylene (up to 100 atm) is added to **4**, nor is there formation of these materials by addition of ethylene to the isolated allyl hydride complexes **2a** and **3a**. Thus, this ethylene oligomerization reaction occurs via some undetected reactive intermediate formed in the initial stages of the reaction. At this point we hesitate to say more about this process since it only appears to be a feature of the ethylene reaction of **1**.

Reaction with Acrylonitrile. The reaction of acrylonitrile with the methylene complex **1** is much more rapid than the ethylene reaction just described. Addition of 1 equiv of acrylonitrile to the methylene complex **1** at −78 °C results in an immediate color change from purple to orange. At −60 °C, all of complex **1** is consumed and an intermediate can be observed that persists indefinitely as long as the temperature is maintained below −40 °C. Above −40 °C, the anti-exo allyl hydride derivative **2b** is observed to grow in and can be isolated in good yield as colorless crystals; in solution, anti-exo **2b** slowly isomerizes to the syn-exo diastereomer **3b** to ultimately generate an approximately 1:1 mixture at equilibrium (in eq 1, R = CN). Recrystallization of the crude equilibrium mixture only produces crystals of anti-exo **2b** in 68% yield. Remarkably, no other stereoisomers (i.e., anti-endo or syn-exo) are observed. Again, assignment of stereochemistry was facilitated by NOE experiments; irradiation of the hydride of the anti-exo isomer **2b** results in no enhancement of the central proton of the allyl unit whereas irradiation of the hydride of the syn-endo isomer **3b** does give a 15% enhancement of the central proton resonance. A notable feature of the NOE experiments of the syn-endo isomer **3b** is the unexpected enhancement of the anti proton of the substituted carbon (H_4) observed when the central proton is irradiated; although the enhancement is small (3–4%), it is reproducible.

The intermediate observed at low temperature corresponds to the isomeric allyl hydride **6b** wherein the hydride is trans to one of the phosphine donors and cis to the other. Although the

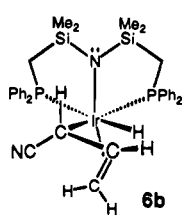

6b

stereochemistry at the iridium center is relatively easy to discern, that is, the tridentate ligand is facial are shown above, the stereochemistry of the substituted allyl unit is speculative. It is assumed that the cyano substituent in **6b** is in the anti position simply because the kinetic isomer **2b** also has this stereochemistry; attempts to use NOE difference experiments to assign an endo or exo orientation of the allyl unit were not successful. In fact, the orientation of the allyl group in both of the intermediates **6a** and **6b** is drawn in the σ-π^2 form to match the conformation of the proposed but unobserved iridacyclobutane intermediate (vide infra).

Another notable difference between the reactions of the methylene complex **1** with ethylene and with acrylonitrile, besides the increased rate of the latter, is the fact that there is no formation of the olefin complex $Ir(\eta^2\text{-}H_2C{=}CHCN)[N(SiMe_2CH_2PPh_2)_2]$; moreover, no oligomerization of acrylonitrile was detected. The only iridium complexes formed in this reaction are the two allyl hydride derivatives **2b** and **3b**.

Other Allyl Hydride Complexes. The other olefins examined that were found to generate allyl hydride complexes were styrene ($H_2C{=}CHPh$), methyl acrylate ($H_2C{=}CHCO_2Me$), and methacrylontrile ($H_2C{=}C(Me)CN$). The reaction of 10 equiv of styrene with the methylene **1** resulted in a slow reaction requiring 12 h to go to completion. In this case only one allyl hydride isomer was detected, and this was determined to be the syn-endo complex **3c** (eq 4). Presumably, this stereoisomer

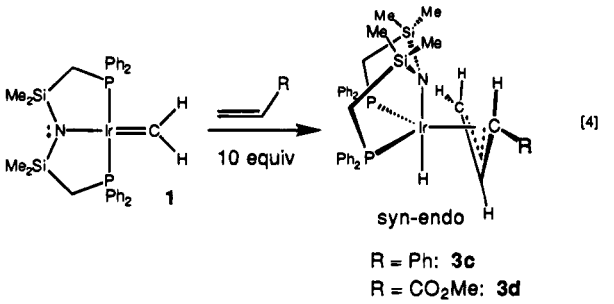

[4]

R = Ph: **3c**
R = CO_2Me: **3d**

is the thermodynamically favored one and the unobserved anti-exo isomer is the kinetically favored isomer, but it is just too unstable to be detected. The methyl acrylate reaction with **1** proceeds at −20 °C as is evidenced by the color change from purple to light yellow. Here again, the only isomer detected is the syn-endo allyl hydride **3d** (eq 4). NOE experiments for **3d** also show the small enhancement of the anti proton H_4 at the substituted carbon when the central proton is irradiated. Curiously, no similar enhancement was observed for the styrene product **3c**.

The reaction of **1** with the disubstituted olefin methacrylonitrile results in the formation of four stereoisomers as evidenced by four triplet Ir–H resonances at −20.18, −20.21, −20.54, and −20.86 ppm in the ^1H NMR spectrum. Two of the four isomers (Ir–H resonances at −20.18 and −20.86 ppm) are formed in only 3–5% of the total crude material and could not be isolated from the reaction mixture; hence, the respective stereochemistries of these two species could not be determined. The major initial product (Ir–H at −20.21 ppm) was shown to be the exo stereoisomer **7** on the basis of NOE experiments; the remaining isomer is presumed to be the endo isomer **8** simply on the basis that it is the one that appears last and grows in at the expense of the exo isomer **7** (eq 5); only $^{31}P\{^1H\}$ NMR spectral data were obtained for **8**. Unfortunately, the resonances of the exo and endo isomers **7** and **8** were sufficiently overlapping that assignment of the stereochemistry of the latter was not possible; thus, the indicated structure of **8** is wishful thinking. Taking speculation even a bit further, the identity of the minor isomers in this reaction could be the same as **7** and

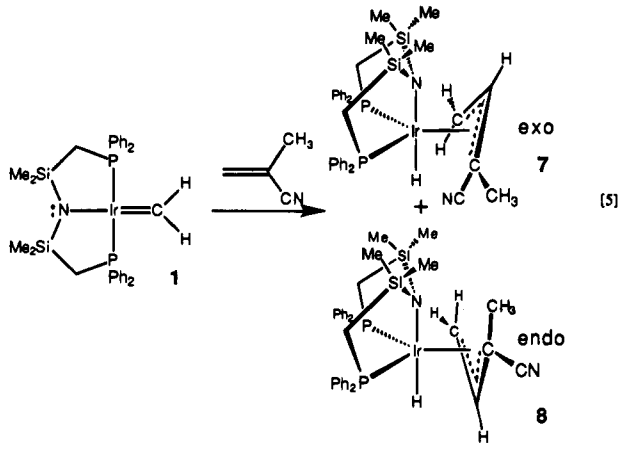

8 except that the methyl and cyano substituents of the respective isomers are reversed.

As already mentioned, there is no reaction between propene and the methylene complex **1**. Clearly this cannot be due simply to steric effects since there is a reaction with methacrylonitrile (eq 5), an olefin that is more sterically crowded than propene. This would suggest that electronic effects are also important. The possibility that the product crotyl hydride complexes that would result from the successful reaction of propene with **1** are intrinsically unstable was shown not to be the case by the synthesis of these compounds by an independent route. Oxidative addition of allyl bromide to the iridium(I) precursor, $Ir(\eta^2\text{-}C_8H_{14})[N(SiMe_2CH_2PPh_2)_2]$, results in the formation of the complex *mer*-$Ir(\eta^3\text{-}C_4H_7)Br[N(SiMe_2CH_2PPh_2)_2]$ (**9**); reaction of the toluene-soluble hydride reagent $KBEt_3H$ with this crotyl bromide derivative results in the formation of the crotyl hydride complexes **2e** and **3e** (eq 6). The stereochemistry of the starting

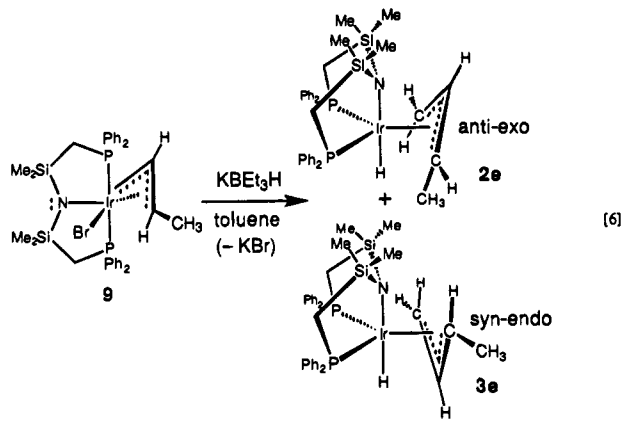

crotyl bromide derivative **9** was shown by NMR spectroscopy and an X-ray crystal structure to have the *mer* geometry at iridium with the *syn*-crotyl ligand.[18] However, upon reaction with a hydride reagent, the stereochemistry at iridium is affected as is the stereochemistry at the substituted allyl carbon. The final product mixture consists of a 1:7 mixture of anti-exo **2e** and syn-endo **3e**. The stereochemistry at iridium is evident from the $^{31}P\{^1H\}$ NMR spectrum of the mixture since each isomer has inequivalent phosphorus-31 nuclei displaying a negligible cis coupling to each other whereas the starting crotyl bromide **9** has trans-disposed inequivalent phosphorus nuclei with a large coupling ($^2J_{PP}$ = 429 Hz). In addition, the hydride pattern for each isomer is a triplet, indicating coupling to two cis-disposed phosphorus nuclei. Identification of the major isomer as syn-

(18) Fryzuk, M. D.; Huang, L.; McManus, N. T.; Paglia, P.; Rettig, S. J.; White, G. S. *Organometallics* **1992**, *11*, 2979.

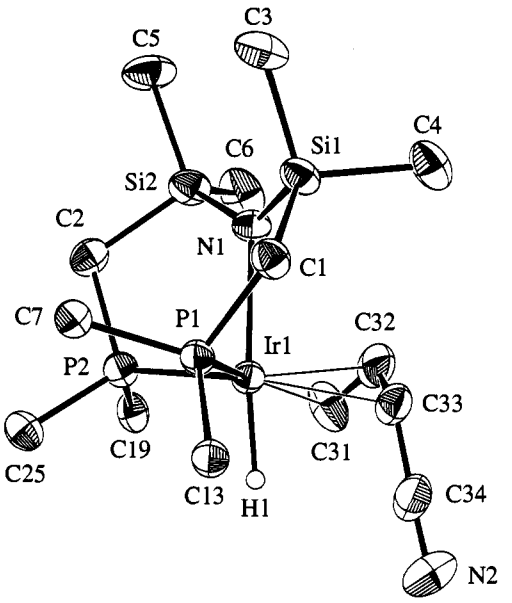

Figure 1. Molecular structure and numbering scheme for the anti-exo complex $Ir(\eta^3\text{-}C_3H_4CN)H[N(SiMe_2CH_2PPh_2)_2]$ (**2b**). For the sake of clarity, only the ipso carbons of the phenyl rings attached to phosphorus have been retained.

endo **3e** was determined from NOE difference type experiments; in particular, irradiation of the central proton on the allyl generates an 8% enhancement on the iridium hydride and a 7% enhancement on the *syn*-methyl protons. Designation of the stereochemistry of the minor isomer as anti-exo is speculative since the resonances of this stereoisomer are somewhat obscured by the major isomer in the ^1H NMR spectrum.

The stability of the crotyl hydride isomers in solution is qualitatively not any different than the other allyl hydride complexes. Thus, one can conclude that it is not the instability of the products that prevents propene from reacting with the methylene complex. A reasonable suggestion is that the olefin binding step is unfavorable because propene is not electron deficient enough to overlap with the relatively electron rich iridium(I) center of **1**.

X-ray Crystal Structure Determinations. Colorless single crystals of the toluene solvate of the anti-exo isomer **2b** from the acrylonitrile reaction were obtained by recrystallization of the crude reaction mixture with a toluene–hexanes mixture. The molecular structure and numbering scheme are shown in Figure 1, important bond lengths are given in Table 2, and a selection of bond angles is listed in Table 3. The tridentate ligand adopts a facial mode of attachment with a P(1)–Ir–P(2) angle of 100.02(4)°. The allyl moiety is arranged exo to the tridentate ligand with the cyano substituent pointing toward the hydride position in the anti position. In the tridentate ligand, the amide nitrogen is very nearly planar, as is evidenced by the sum of the three angles Ir–N(1)–Si(1), 112.8(2)°, Ir–N(1)–Si(2), 111.9(2)°, and Si(1)–N(1)–Si(2), 133.7(2)°, totaling to 356.6°. The allyl unit is distorted since the cyano substituent is not in the plane defined by the three allyl carbons C(31), C(32), and C(33); C(34) lies 0.766 Å out of the plane away from the iridium center with a torsion angle for C(31)–C(32)–C(33)–C(34) of 39.9(8)°. The bond distances in the allyl unit are quite different as follows: C(31)–C(32) is 1.376(7) Å and C(32)–C(33) is 1.430(7) Å; this indicates a distortion toward $\sigma\text{-}\pi^2$ with the pivot σ-bond at the substituted carbon. The hydride ligand attached to iridium was located in the difference map: the Ir–H(1) bond length is 1.54 Å.

Colorless single crystals of the syn-endo crotyl hydride isomer **3e** were obtained from hexanes at room temperature; the

molecular structure and numbering scheme are shown in Figure 2, while important bond lengths and bond angles can be found in Tables 2 and 3, respectively. The ancillary tridentate ligand is again found in the facial mode of attachment with a slightly larger (than **2b**) P(1)−Ir−P(2) angle of 105.02(4)°. In this structure, the allyl unit is endo; that is, the central C−H unit points underneath the tridentate ligand, toward the hydride position trans to the amide nitrogen. In **3e**, the amide nitrogen of the tridentate ligand is closer to being planar than in **2b**, as is evidenced by the sum of the three angles Ir−N(1)−Si(1), 114.2(3)°, Ir−N(1)−Si(2), 111.9(3)°, and Si(1)−N(1)−Si(2), 132.7(4)°, totaling to 358.8°, versus 356.6° for **2b**. The crotyl unit is **3e** is not distorted at the substituted carbon as was found for **2b**, since all four carbons are found to lie on a plane within experimental error; the methyl substituent on the allyl unit is clearly in the syn orientation. The bond distances in the allyl unit of **3e** are slightly different as follows: C(31)−C(32) is 1.33(1) Å and C(32)−C(33) is 1.45(1) Å, similar to that found for anti-exo **2b** above further evidence for a distortion toward σ-π^2 with the pivot σ-bond at the substituted carbon. The hydride ligand attached to iridium was refined isotropically, and the Ir−H(1) bond length is 1.74(5) Å. All of the other bond lengths and angles are similar to those of related complexes and show no obvious discrepancies.

An important complex to mention is the iridium(III) allyl hydride complex shown below.[19] This derivative was formed

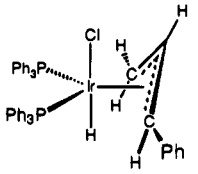

syn-exo

by the reaction of phenylcyclopropane with an Ir(I) precursor and was characterized crystallographically. Two aspects are noteworthy: first, there is again a distortion toward σ-π^2 with the pivot σ-bond at the substituted carbon (distances are 1.378(12) and 1.427(8) Å) and, second, the observed stereochemistry is syn-exo, a geometry not found for the reaction of olefins with the methylene complex **1**.

Mechanism of Formation of Allyl Hydride Complexes. On the basis of the observed intermediates in the ethylene and acrylonitrile reactions with the methylene **1**, the mechanism in Scheme 2 is suggested. The first step in the proposed mechanism is binding of the olefin to the iridium(I) methylene **1** to form the intermediate **5**; for R = H, this species was detected and proposed to have the indicated structure largely on the basis of an upfield shift of the methylene resonance and equivalent phosphorus-31 nuclei. Rearrangement of **5** to the iridacyclobutane **10** is proposed to analogy to metathesis-type reactions; however, in this case, the four-membered ring is suggested to be rather puckered since this would facilitate β-elimination from the central carbon to the open site at the iridium center trans to one of the phosphorus donors to generate the observed intermediate **6**. For both **6a** (R = H) and **6b** (R = CN), this intermediate was characterized as having the hydride trans to one phosphorus and cis to the other. The indicated arrangement of the allyl group in **6** as σ-π^2 with the pivot at the substituted end of the allyl unit was not substantiated spectroscopically; however, this particular bonding mode would facilitate the rearrangement to the presumed kinetic anti-exo isomer **2** by simple interchange of the hydride and the olefin ligands. The other possible σ-π^2 formulation, shown below as **6′**, cannot be entirely ruled out; however, we note that all of the structural data on the final products support the former proposal.

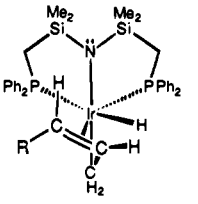

6′

The subsequent rearrangement of the anti-exo isomer **2** to the thermodynamically more stable syn-endo form **3** occurs via a standard σ-π rearrangement with the pivot σ-bond forming at the substituted end of the allyl ligand. The relative stabilities of the anti-exo and syn-endo stereoisomers, i.e., **2** and **3**, for the different substituents R are not easily rationalized. For the relatively small substituents R = H and R = CN, nearly equal amounts of these stereoisomers are observed at equilibrium; however, as the substituents increase in size, the syn-endo stereoisomer predominates to the extent that for R = Ph and CO_2Me none of the anti-exo form could be detected.

The stereoselectivity of this reaction is remarkable. The reaction of a monosubstituted olefin with the iridium methylene complex **1** could, in principle, generate four diastereomeric allyl hydride complexes: the exo form with the substituent anti or syn and the endo form with the substituent anti or syn. The mechanism shown in Scheme 2 attempts to rationalize this stereoselectivity through the formation of the olefin adduct of the methylene complex, **5**; by having the substituent on the olefin pointing down and away from the ligand backbone, i.e., **5**, one avoids the steric repulsion that would occur by coordination of the other enantiotopic face with the substituent R pointing toward the silyl methyls to generate the diastereomer **5′**. Once

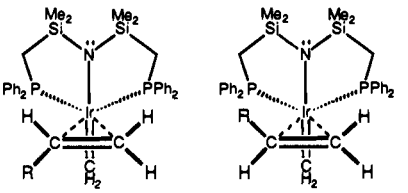

5 **5′**

the olefin adduct **5** is formed, all of the subsequent steps in the mechanism in Scheme 2 are stereocontrolled to generate only the anti-exo diastereomer **2**. These arguments are not easily substantiated since the only olefin adduct detected spectroscopically is **5a** (R = H) and it is stereochemically trivial. However, if the diastereomer **5′** did form, then the mechanism in Scheme 2 would cascade to produce the unobserved syn-exo diastereomer as the kinetic isomer. Since it is not observed, the diastereoselectivity of the olefin binding step to give **5** and not **5′** is consistent with the observed stereoselectivity of the reaction.

There are two steps in the proposed mechanism shown in Scheme 2 that deserve further discussion since they are controversial and one step is somewhat unconventional. The olefin addition to **1** to generate **5** is unconventional since one would normally expect the olefin and the metal−carbon double bond to line up in a collinear fashion[20−22] rather than the proposed perpendicular mode as shown in Scheme 3. However, as is suggested by the orbitals displayed in Scheme 3, the perpendicular mode could be favored if there was an available

(19) Tulip, T. H.; Ibers, J. A. *J. Am. Chem. Soc.* **1979**, *101*, 4201.

Table 1. Crystallographic Data[a]

compound	$[(Ph_2PCH_2SiMe_2)_2N]Ir(H)(\eta^3$-$C_3H_4CN)$·$C_6H_5CH_3$, **2b**	$[(Ph_2PCH_2SiMe_2)_2N]Ir(H)(\eta^3$-$C_3H_4CH_3)$, **3e**
formula	$C_{34}H_{41}IrN_2P_2Si_2$·C_7H_8	$C_{34}H_{44}IrNP_2Si_2$
fw	880.19	777.07
color, habit	colorless, prism	colorless, prism
crystal size, mm	0.25 × 0.40 × 0.40	0.15 × 0.25 × 0.40
crystal system	monoclinic	monoclinic
space group	$P2_1/c$	$P2_1/n$
a, Å	10.884(1)	13.606(2)
b, Å	18.672(2)	14.687(4)
c, Å	20.169(3)	17.672(3)
β°	100.32(2)	100.86(1)
V, Å^3	4032.8(8)	3467(1)
Z	4	4
T, °C	21	21
D_c, g/cm^3	1.449	1.488
$F(000)$	1776	1560
μ(Mo K_α), cm^{-1}	34.64	40.45
transmission factors	0.62−1.00	0.70−1.00
scan type	ω−2θ	ω−2θ
scan range, deg in ω	1.31 + 0.35 tan θ	1.26 + 0.35 tan θ
scan speed, deg/min	16 (up to 8 rescans)	32 (up to 8 rescans)
data collected	$+h, +k, \pm l$	$+h, +k, \pm l$
$2\theta_{max}$, deg	60	55
crystal decay	negligible	negligible
total no. of reflns	12 668	8587
unique reflns	12 076	8243
R_{merge}	0.047	0.034
no. with $I \geq 3\sigma(I)$	6304	4226
no. of variables	434	366
R	0.032	0.034
R_w	0.028	0.033
gof	1.74	1.97
max Δ/σ (final cycle)	0.18[b]	0.07
residual density e/Å^3	−0.82, 0.84 (near lR)	−0.63, 0.76 (near lR)

[a] Rigaku AFC6S diffractometer, Mo $K\alpha$ radiation, λ = 0.71069 Å, graphite monochromator, takeoff angle 6.0°, aperture 6.0 × 6.0 mm at a distance of 285 mm from the crystal, stationary background counts at each end of the scan (scan/background time ratio 2:1), $\sigma^2(F^2) = [S^2(C + 4B)]/Lp^2$ (S = scan speed, C = scan count, B = normalized background count), function minimized $\sum w(|F_o| - |F_c|)^2$ where $w = 4F_o^2/\sigma^2(F_o^2)$, $R = \sum||F_o| - |F_c||/\sum|F_o|$, $R_w = (\sum w(|F_o| - |F_c|)^2/\sum w|F_o|^2)^{1/2}$, and gof = $[\sum w(|F_o| - |F_c|)^2/(m - n)]^{1/2}$. Values given for R, R_w, and gof are based on those reflections with $I \geq 3\sigma(I)$. [b] Associated with the solvent molecule, all parameter shifts for the metal complex were less than 0.04σ.

Table 2. Selected Bond Lengths (Å) with Estimated Standard Deviations

atoms	distance	atoms	distance
anti-exo-Ir(η^3-C_3H_4CN)H[N($SiMe_2CH_2PPh_2$)$_2$] (**2b**·C_7H_8)			
Ir(1)−P(1)	2.283(1)	Si(1)−N(1)	1.685(4)
Ir(1)−P(2)	2.274(1)	Si(1)−C(1)	1.904(4)
Ir(1)−N(1)	2.257(3)	Si(1)−C(3)	1.896(5)
Ir(1)−C(31)	2.265(5)	Si(1)−C(4)	1.885(5)
Ir(1)−C(32)	2.139(5)	Si(2)−C(2)	1.696(4)
Ir(1)−C(33)	2.243(5)	Si(2)−C(5)	1.908(5)
Ir(1)−H(1)	1.54	Si(2)−C(6)	1.870(5)
P(1)−C(1)	1.812(4)	Si(2)−C(16)	1.870(6)
P(1)−C(7)	1.828(4)	N(2)−C(34)	1.146(6)
P(1)−C(13)	1.822(4)	C(31)−C(32)	1.376(7)
P(2)−C(2)	1.815(5)	C(32)−C(33)	1.430(7)
P(2)−C(19)	1.840(5)	C(33)−C(34)	1.406(7)
P(2)−C(25)	1.832(5)		
syn-endo-Ir(η^3-C_3H_4Me)H[N($SiMe_2CH_2PPh_2$)$_2$] (**3e**)			
Ir(1)−P(1)	2.280(2)	P(2)−C(25)	1.854(8)
Ir(1)−P(2)	2.277(2)	Si(1)−N(1)	1.689(6)
Ir(1)−N(1)	2.281(5)	Si(1)−C(1)	1.906(7)
Ir(1)−C(31)	2.221(8)	Si(1)−C(3)	1.852(9)
Ir(1)−C(32)	2.161(8)	Si(1)−C(4)	1.899(9)
Ir(1)−C(33)	2.238(8)	Si(2)−C(2)	1.676(6)
Ir(1)−H(1)	1.74(5)	Si(2)−C(5)	1.912(7)
P(1)−C(1)	1.814(7)	Si(2)−C(6)	1.866(9)
P(1)−C(7)	1.854(7)	Si(2)−C(16)	1.876(8)
P(1)−C(13)	1.821(7)	C(31)−C(32)	1.33(1)
P(2)−C(2)	1.827(6)	C(32)−C(33)	1.45(1)
P(2)−C(19)	1.819(7)	C(33)−C(34)	1.41(1)

filled nonbonding d-type orbital on the metal fragment that could overlap with the π^* orbital of the incoming olefin.

We have performed semiempirical molecular orbital calculations at the INDO-1 level using ZINDO on the CAChe Worksystem. In Figure 3 we show the results of this performed on the rhodium-based fragment $Rh{=}CH_2(NH_2)(PH_3)_2$ with a P−Rh−P angle of 100° to match that found in the structure determinations; the Rh is used because there are no parameters for Ir or any other third-row element. In the bent mode, the HOMO is indeed a filled d-like orbital that provides the correct symmetry overlap for the perpendicular mode of binding of the olefin. As it turns out, HOMO-1 has the appropriate symmetry for the collinear binding of the olefin while HOMO-2 and HOMO-3 are essentially d orbitals (d_{xy} and d_{z^2}, respectively). For the sake of completeness, we include HOMO-4 and HOMO-5 which are the extended π-type orbitals that result from amide overlap with the metal−carbon double bond; these last orbitals are essentially as shown except that they differ in their parities.

Interestingly, when the same level of calculations was performed on the square-planar rhodium-based fragment $Rh{=}CH_2(NH_2)(PH_3)_2$ with a P−Rh−P angle now of 180°, the ordering of the orbitals changed such that now the HOMO (at −8.509 eV) was the $Rh{=}CH_2$ double bond similar to that of HOMO-1 in Figure 3, therefore having the appropriate symmetry for the collinear binding. In the planar form, the d-like orbital

(20) Eisenstein, O.; Hoffmann, R.; Rossi, A. R. *J. Am. Chem. Soc.* **1981**, *103*, 5582.
(21) Kress, J.; Osborn, J. A. *Angew. Chem., Int. Ed. Engl.* **1992**, *31*, 1585.
(22) Youinou, M. T.; Kress, J.; Fischer, J.; Aguero, A.; Osborn, J. A. *J. Am. Chem. Soc.* **1988**, *110*, 1488.

Table 3. Selected Bond Angles (deg) with Estimated Standard Deviations

atoms	angle	atoms	angle
anti-exo-Ir(η^3-C_3H_4CN)H[N($SiMe_2CH_2PPh_2$)$_2$] (**2b**·C_7H_8)			
P(1)–Ir(1)–P(2)	100.02(4)	Ir(1)–P(2)–C(19)	112.4(2)
P(1)–Ir(1)–N(1)	82.06(9)	Ir(1)–P(2)–C(25)	118.8(2)
P(1)–Ir(1)–C(31)	163.0(2)	C(2)–P(2)–C(19)	107.6(2)
P(1)–Ir(1)–C(32)	129.7(2)	C(2)–P(2)–C(25)	107.4(2)
P(1)–Ir(1)–C(33)	97.0(1)	C(19)–P(2)–C(25)	100.6(2)
P(1)–Ir(1)–H(1)	98.9	N(1)–Si(1)–C(1)	105.7(2)
P(2)–Ir(1)–N(1)	88.67(9)	N(1)–Si(1)–C(3)	116.9(2)
P(2)–Ir(1)–C(31)	96.6(2)	N(1)–Si(1)–C(4)	115.6(2)
P(2)–Ir(1)–C(32)	128.0(2)	C(1)–Si(1)–C(3)	108.6(2)
P(2)–Ir(1)–C(33)	162.2(1)	C(1)–Si(1)–C(4)	106.7(2)
P(2)–Ir(1)–H(1)	96.4	C(3)–Si(1)–C(4)	102.9(2)
N(1)–Ir(1)–C(31)	102.2(2)	N(1)–Si(2)–C(2)	105.7(2)
N(1)–Ir(1)–C(32)	84.7(2)	N(1)–Si(2)–C(5)	116.5(2)
N(1)–Ir(1)–C(33)	98.8(2)	N(1)–Si(2)–C(6)	114.1(2)
N(1)–Ir(1)–H(1)	174.6	C(2)–Si(2)–C(5)	105.0(2)
C(31)–Ir(1)–C(32)	36.3(2)	C(2)–Si(2)–C(5)	109.6(2)
C(31)–Ir(1)–C(33)	66.2(2)	C(5)–Si(2)–C(6)	105.5(3)
C(31)–Ir(1)–H(1)	75.4	Ir(1)–N(1)–Si(1)	112.8(2)
C(32)–Ir(1)–C(33)	38.0(2)	Ir(1)–N(1)–Si(2)	111.9(2)
C(32)–Ir(1)–H(1)	90.7	Si(1)–N(1)–Si(2)	133.7(2)
C(33)–Ir(1)–H(1)	75.8	C(33)–C(34)–N(2)	177.5(7)
Ir(1)–P(1)–C(1)	105.4(1)	Ir(1)–C(31)–C(32)	66.9(3)
Ir(1)–P(1)–C(7)	120.5(1)	Ir(1)–C(32)–C(31)	76.9(3)
Ir(1)–P(1)–C(13)	118.7(2)	Ir(1)–C(32)–C(33)	74.9(3)
C(1)–P(1)–C(7)	104.6(2)	C(31)–C(32)–C(33)	122.6(5)
C(1)–P(1)–C(13)	104.3(2)	Ir(1)–C(33)–C(32)	67.1(3)
C(7)–P(1)–C(13)	101.5(2)	Ir(1)–C(33)–C(34)	112.5(4)
Ir(1)–P(2)–C(2)	109.3(2)	C(32)–C(33)–C(34)	121.9(5)
syn-endo-Ir(η^3-C_3H_4Me)H[N($SiMe_2CH_2PPh_2$)$_2$] (**3e**)			
P(1)–Ir(1)–P(2)	105.98(7)	Ir(1)–P(2)–C(19)	121.1(2)
P(1)–Ir(1)–N(1)	84.1(2)	Ir(1)–P(2)–C(25)	113.2(2)
P(1)–Ir(1)–C(31)	157.9(2)	C(2)–P(2)–C(19)	106.2(3)
P(1)–Ir(1)–C(32)	125.4(3)	C(2)–P(2)–C(25)	105.4(3)
P(1)–Ir(1)–C(33)	91.9(3)	C(19)–P(2)–C(25)	98.7(3)
P(1)–Ir(1)–H(1)	97(1)	N(1)–Si(1)–C(1)	107.2(3)
P(2)–Ir(1)–N(1)	87.7(1)	N(1)–Si(1)–C(3)	115.3(4)
P(2)–Ir(1)–C(31)	96.0(2)	N(1)–Si(1)–C(4)	116.6(4)
P(2)–Ir(1)–C(32)	126.0(3)	C(1)–Si(1)–C(3)	107.6(4)
P(2)–Ir(1)–C(33)	161.9(3)	C(1)–Si(1)–C(4)	105.9(4)
P(2)–Ir(1)–H(1)	96(1)	C(3)–Si(1)–C(4)	103.5(4)
N(1)–Ir(1)–C(31)	94.4(3)	N(1)–Si(2)–C(2)	106.9(3)
N(1)–Ir(1)–C(32)	110.9(3)	N(1)–Si(2)–C(5)	115.5(4)
N(1)–Ir(1)–C(33)	91.3(3)	N(1)–Si(2)–C(6)	115.5(4)
N(1)–Ir(1)–H(1)	175(1)	C(2)–Si(2)–C(5)	110.1(4)
C(31)–Ir(1)–C(32)	35.3(3)	C(2)–Si(2)–C(5)	104.3(3)
C(31)–Ir(1)–C(33)	66.1(3)	C(5)–Si(2)–C(6)	103.9(4)
C(31)–Ir(1)–H(1)	82(1)	Ir(1)–N(1)–Si(1)	114.2(3)
C(32)–Ir(1)–C(33)	38.5(3)	Ir(1)–N(1)–Si(2)	111.9(3)
C(32)–Ir(1)–H(1)	64(1)	Si(1)–N(1)–Si(2)	132.7(4)
C(33)–Ir(1)–H(1)	84(1)	Ir(1)–C(31)–C(32)	69.9(5)
Ir(1)–P(1)–C(1)	106.3(2)	Ir(1)–C(32)–C(31)	74.8(5)
Ir(1)–P(1)–C(7)	120.0(2)	Ir(1)–C(32)–C(33)	73.6(5)
Ir(1)–P(1)–C(13)	118.2(2)	C(31)–C(32)–C(33)	121(1)
C(1)–P(1)–C(7)	103.4(3)	Ir(1)–C(33)–C(32)	67.9(5)
C(1)–P(1)–C(13)	104.5(3)	Ir(1)–C(33)–C(34)	129.2(8)
C(7)–P(1)–C(13)	102.6(3)	C(32)–C(33)–C(34)	123.6(10)
Ir(1)–P(2)–C(2)	110.6(2)		

appropriate for generation of the perpendicular binding was HOMO-3 at −10.109 eV. As has been argued previously,[20] while the collinear binding would be expected to lead directly to the metallacyclobutane, in this case, it must involve disruption of this amido–metal–carbon double-bond π-system.

This brings the discussion to the other controversial proposal in Scheme 2, the formation of a puckered metallacyclobutane from an intermediate that has the olefin perpendicular to the iridium–methylene π-system. The suggestion has always been that a collinear approach of the olefin π^* orbitals is necessary for ring formation via cycloaddition, particularly as applied to olefin metathesis.[21,22] What we would propose is that, for the

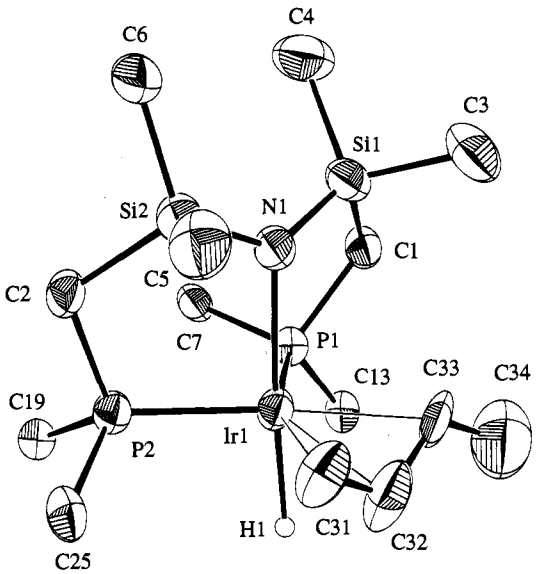

Figure 2. Molecular structure and numbering scheme for the syn-endo complex Ir(η^3-C_3H_4Me)H[N($SiMe_2CH_2PPh_2$)$_2$] (**3e**). For the sake of clarity, only the ipso carbons of the phenyl rings attached to phosphorus have been retained.

iridium complex **1**, formation of the metallacyclobutane ring occurs via a migratory insertion reaction of the methylene into an iridium–carbon bond. In other words, the perpendicular approach of the olefin to generate **5** in Scheme 2 generates not a simple olefin adduct of Ir(I) but rather an iridacyclopropane with the metal center now formally Ir(III) as shown in **5″** below.

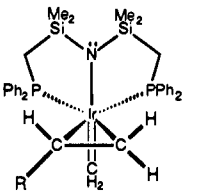

5″

Such a formulation not only obviates the collinear geometry requirement but is also consistent with the fact that this reaction is more facile with electron-deficient olefins. As the substituent R is electron-withdrawing, this migratory insertion can alternatively be represented as a Michael addition of the somewhat nucleophilic methylene unit to the terminus of the coordinated olefin.

One last point is that we observe no metathesis-type reactions with this iridium–methylene complex, only the formation of allyl hydride derivatives, the presumed intermediate in the homologation of olefins via path **c** in Scheme 1. Yet there are reports of late metal catalysts that can act as precursors to olefin metathesis catalysts. Two notable examples are the Ru(II) complex **11**[23,24] and a poorly characterized iridium(III) species formed by in-situ oxidation of Ir(I) with Ag(OTf).[25] One obvious

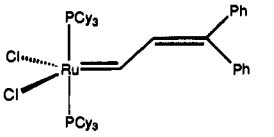

11

difference is that these latter two systems have Ru(II) and Ir(III) metal centers, both of which are d^6, while the methylene

Scheme 2

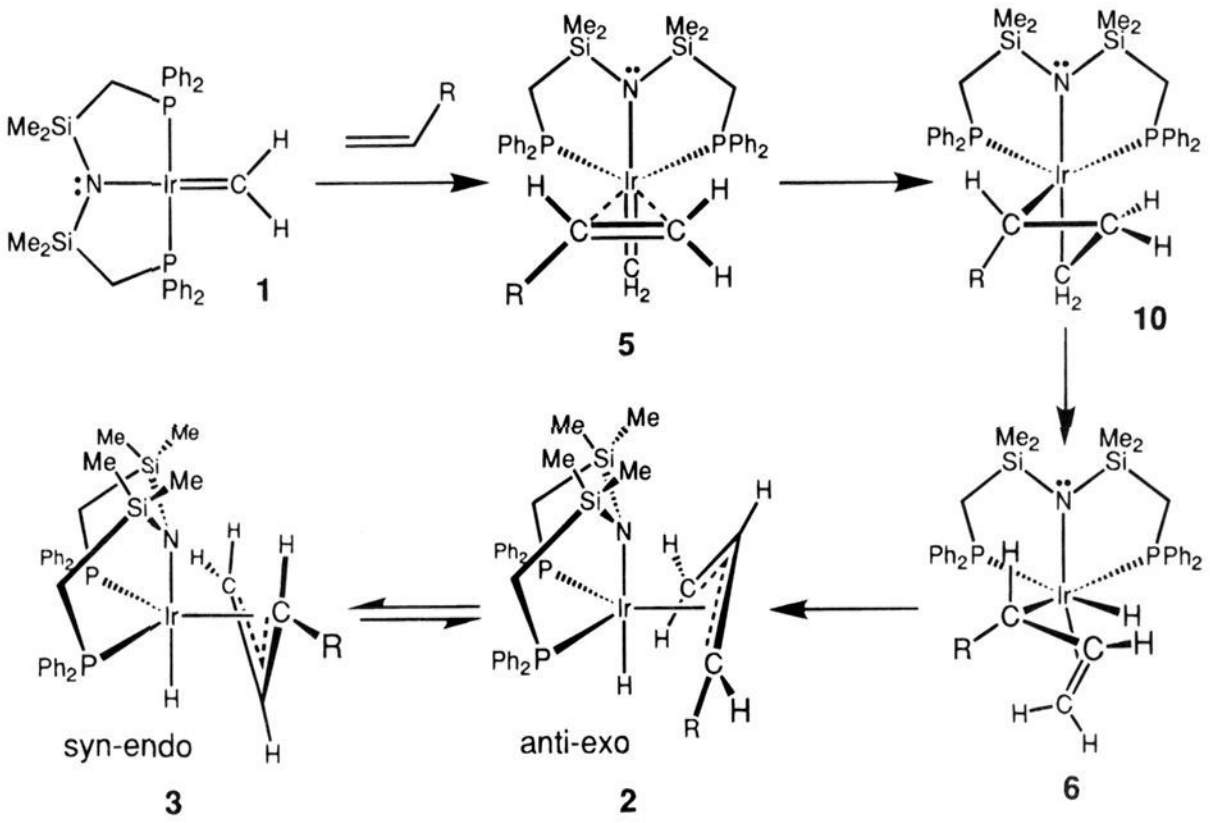

Scheme 3

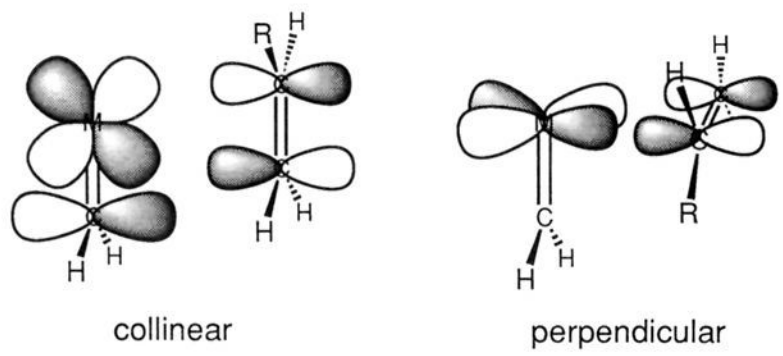

complex **1** is formally Ir(I) and therefore d^8. The extra two electrons in **1** are required for the perpendicular binding of olefins as shown in Scheme 3; without these two electrons, one can anticipate that the collinear binding is now favored and a planar metallacyclobutane intermediate is the result. If the puckered metallacyclobutane leads to β-elimination as the preferred reaction mode, whereas a planar four-membered ring leads to olefin metathesis, then a simple rationale is available for understanding this dichotomy in reactivity. However, this is clearly too simple-minded since it is known that formally d^6 Pt(IV) platinacyclobutanes,[6] generated by cyclopropane addition to Pt(II) complexes, have slightly puckered ring structures and decompose and rearrange via other mechanisms, not necessarily by β-elimination. Clearly, ligand and metal effects are important but not precisely understood.[5]

Experimental Section

General Procedures. Details of general procedures have already been detailed.[12] Acrylonitrile, ethyl vinyl ether, styrene, methyl acrylate, and methacrylonitrile were distilled over molecular sieves and collected over molecular sieves; ethylene and propene were used as received.

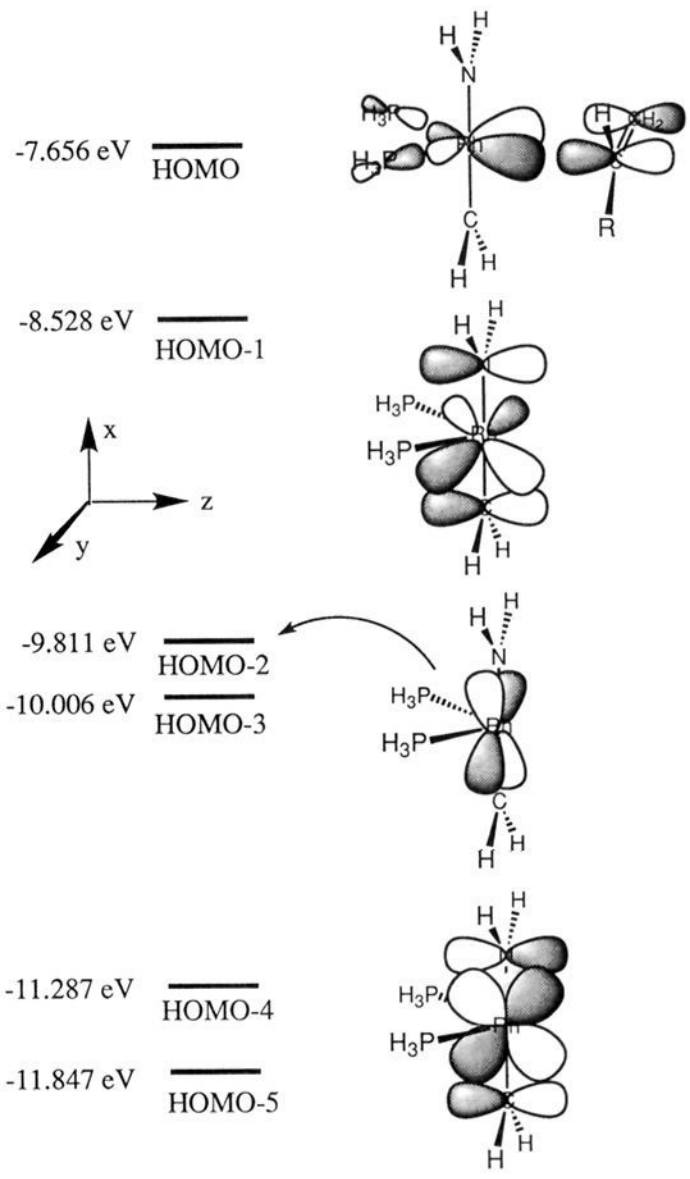

Figure 3. Molecular oribtal scheme (ZINDO) for the fragment $Rh{=}CH_2(NH_2)(PH_3)_2$; only the HOMO to HOMO-5 levels are shown. The HOMO is shown with the π^* orbital of the olefin in the perpendicular mode to illustrate the potential overlap.

$KBEt_3H$ was recrystallized from toluene before use. Deuterated methyl iodide (CD_3I, 99.5%) and ^{13}C-labeled methyl iodide ($^{13}CH_3I$, 99.7%) were purchased from MSD Isotopes, degassed prior to use, and stored over molecular sieves and a small amount of copper powder in the dark. The complexes $Ir{=}CH_2[N(SiMe_2CH_2PPh_2)_2]$, $Ir{=}CD_2[N(SiMe_2CH_2PPh_2)_2]$, and $Ir{=}^{13}CH_2[N(SiMe_2CH_2PPh_2)_2]$ were prepared as previously described[1,2] starting from $Ir(CH)_3I[N(SiMe_2CH_2PPh_2)_2]$, $Ir(CD_3)I[N(SiMe_2CH_2PPh_2)_2]$, and $Ir(^{13}CH_3)I[N(SiMe_2CH_2PPh_2)_2]$, respectively. GC-MS spectra were recorded on a CARLO ERBA/

(23) Fu, G. C.; Nguyen, S. T.; Grubbs, R. H. *J. Am. Chem. Soc.* **1993**, *115*, 9856.
(24) Nguyen, S. T.; Grubbs, R. H.; Ziller, J. W. *J. Am. Chem. Soc.* **1993**, *115*, 9858.
(25) France, M. B.; Feldman, J.; Grubbs, R. H. *J. Chem. Soc., Chem. Commun.* **1994**, 1307.
(26) *teXsan*: Crystal Structure Analysis Package; Molecular Structure Corporation: The Woodlands, TX, 1985 and 1992.
(27) (a) *International Tables for Crystallography*, Vol. IV; The Kynoch Press: Birmingham, U.K. (present distributor: Kluwer Academic Publishers: Boston, MA), 1974; pp 99−102. (b) *International Tables for Crystallography*, Vol. C; Kluwer Academic Publishers: Boston, MA, 1992; pp 219−222.

Chart 1

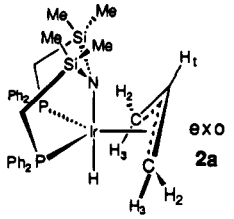

		^1H	$^1H\{^{31}P\}$	
PPh_2	para	7.84-7.73 (m)	m	
	meta/ortho	7.25-6.95 (m,)	m	
H_1		4.17 (m)	tt	$^3J_{HH}$ = 7 Hz, $^3J_{HH}$ = 11.5 Hz
H_2		3.06 (m)	d	$^3J_{HH}$ = 7.0 Hz
H_3		2.80 (dd)	d	$^3J_{HH}$ = 12.0 Hz, $^3J_{PH}$ = 6.0 Hz
$SiCH_2P$		1.75 (dd)	d	$^3J_{PH}$ = 13.9 Hz, $^3J_{HH}$ = 14.0 Hz
$SiCH_2P$		1.70 (dd)	d	$^3J_{PH}$ = 13.9 Hz, $^3J_{HH}$ = 14.0 Hz
SiMe		0.63 (s)	s	
SiMe		0.16 (s)	s	
Ir-H		-21.12 (t)	s	$^3J_{PH}$ = 13.0 Hz

$^{31}P\{^1H\}$: 6.14 (s)

NOE Experiment

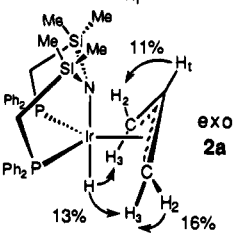

Fractovap series 4160 chromatograph equipped with a KRATOS MS80 RFA double-focusing mass spectrometer and a KRATOS DS 55 data system. The columns used were either DB1-15, 30 M (0.25 μm) or DB1-15, 15 M (0.25 μM). All molecular orbital calculations were performed on a Macintosh IIx using the ZINDO program, part of the CAChe Scientific workstation software and hardware. The parameters for the atoms of $Rh{=}CH_2(NH_2)(PH_3)_2$ were taken from the literature;[28] the model was constructed with C_s symmetry using the following bond distances and bond angles: Rh–C, 1.868 Å; Rh–N, 2.080 Å; Rh–P, 2.288 Å; C–H, 1.090 Å; N–H, 1.070 Å; P–H, 1.380 Å; P–Rh–P, 100.0°; C–Rh–N, 180.0°.

Preparation of Ir(η^3-C_3H_5)H[N($SiMe_2CH_2PPh_2$)$_2$] (2a). To a toluene solution (15 mL) of the methylene complex **1** (100 mg, 0.136 mmol) in a glass bomb (30 mL) was added ethylene at 1 atm. The solution was stirred for 36 h at room temperature during which time the characteristic, deep purple color of **1** slowly discharged to give a yellow solution. The solvent was pumped to dryness, and the residue was dissolved in hexanes (3 mL). Slow evaporation to almost dryness gave colorless needle crystals, which were washed with cold hexanes to remove the yellow Ir(η^2-C_2H_4)[N($SiMe_2CH_2PPh_2$)$_2$] (**4**) and then were dried under vacuum. Yield of complex **2a** (Chart 1): 49 mg (47%). Anal. Calcd for $C_{33}H_{42}IrNP_2Si_2$: C, 51.95; H, 5.55; N, 1.84. Found: C, 51.78; H, 5.39; N, 1.74. $^{31}P\{^1H\}$ NMR (C_6D_6, δ): 6.14 (s). Exo complex **2a** isomerizes to the endo isomer **3a** in solution (Chart 2). $^{31}P\{^1H\}$ NMR of complex **3a** (C_6D_6, δ): 9.31 (s).

Preparation of Samples for GC-MS Spectra. The solution, after the reaction between complex **1** and ethylene was completed, was passed very slowly through two columns of basic alumina (each was 1.5 cm long). The colorless filtrate was concentrated by blowing with nitrogen and then injected into the GC column.

Preparation of Ir(η^3-$CH_2CHCHCN$)H[N($SiMe_2CH_2PPh_2$)$_2$] (2b and 3b). To a frozen solution (LN_2) of the methylene complex **1** (80 mg, 0.109 mmol) in toluene (10 mL) was added acrylonitrile (5 equiv). The solution was allowed to warm up to room temperature with stirring to generate a slightly yellow solution. The toluene and excess acrylonitrile were removed in vacuo, and the remaining tarry residue was dissolved in a minimum amount of toluene. Slow evaporation of the solvent gave colorless crystals of complex *anti-exo*-**2b** (Chart 3),

(28) Anderson, W. P.; Cundari, T. R.; Drago, R. S.; Zerner, M. C. *Inorg. Chem.* **1990**, *29*, 1.

Chart 2

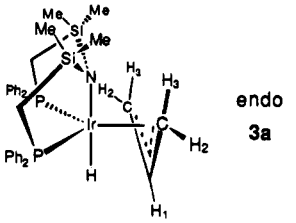

		^1H	$^1H\{^{31}P\}$	J
PPh_2	para	7.71-7.58 (m)	m	
	meta/ortho	6.78-6.55 (m,)	m	
H^1		5.34 (m)	tt	$^3J_{HH}$ = 6.3 Hz, $^3J_{HH}$ = 10.0 Hz; $^3J_{PH}$ = ?
H^2		2.74 (quasi d)	d	$^3J_{HH}$ = 6.3 Hz, $^3J_{PH}$ = ?
H^3		2.13 (dd),	d	$^3J_{HH}$ = 10.0 Hz, $^3J_{PH}$ = 7.6 Hz
$SiCH_2P$		1.88, 1.83 (dd),	d	$^3J_{HH}$ = 14.0 Hz, $^3J_{PH}$ = 11.5 Hz
SiMe		0.72, 0.27 (s)	s	
Ir-H		-21.78 (t)	s	$^3J_{PH}$ = 11.3 Hz

$^{31}P\{^1H\}$: 9.31 (s)

NOE Experiment

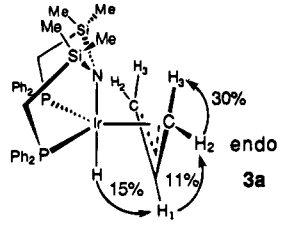

Chart 3

4.9 Hz), 9.72 (d, $^2J_{PP}$ = 4.9 Hz).

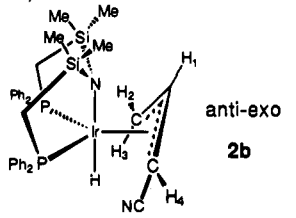

		^1H	$^1H\{^{31}P\}$	J
PPh_2	para	8.1 (m), 7.6 (m)		
		7.4 (m), 7.1 (m)		
	meta/ortho	7.1(m), 6.6 (m)		
H^1		4.23 (m)	br. q	
H^2		2.96 (br. d)	d	$^3J_{HH}$ = 6.3 Hz
H^3		3.64 (br. d)	d	$^3J_{HH}$ = 10.9 Hz
H^4		3.29 (br. s)	br. s	
$SiCH_2P$		1.76, 1.53 (t)	d	$^3J_{PH}$ = 13.8 Hz, $^3J_{HH}$ = 13.8 Hz
$SiCH_2P$		1.62, 1.40 (t)	d	$^3J_{PH}$ = 14.0 Hz, $^3J_{HH}$ = 14.0 Hz
SiMe		0.56, 0.54, -0.28	s	
Ir-H		-19.30 (t)	s	$^3J_{PH}$ = 13.3 Hz

$^{31}P\{^1H\}$: 4.14 (s)

NOE Experiment

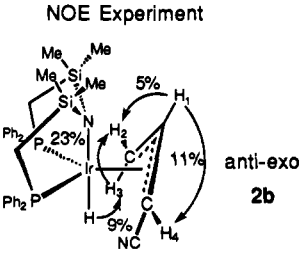

which were washed with cold toluene (−40 °C, 1 mL) and then cold hexanes (−40 °C, 3 × 1 mL) and dried briefly under vacuum. Yield: 63 mg (66%). Anal. Calcd for $C_{34}H_{41}IrN_2P_2Si_2{\cdot}C_7H_8$: C, 55.94; H, 5.61; N, 3.18. Found: C, 55.64; H, 5.72; N, 3.50. $^{31}P\{^1H\}$ NMR (C_6D_6, δ): 4.14 (s). Complex **2b** isomerizes to complex **3b** in solution (Chart 4). $^{31}P\{^1H\}$ NMR spectrum of **3b** (C_6D_6, δ): 7.20 (d, $^2J_{PP}$ = 4.9 Hz), 9.72 (d, $^2J_{PP}$ = 4.9 Hz).

Chart 4

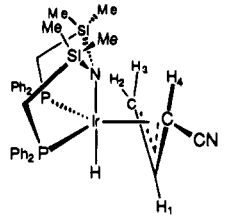

syn-endo
3b

	^{1}H	^{1}H(^{31}P)	J
PPh_2	obscured		
H^1	5.42 (br.dd)	br.dd	
H^4	2.60 (t)	d	$^3J_{HH}$ = 8.0 Hz, $^3J_{PH}$ =8.0 Hz
H^2	2.16 (m),	d	$^3J_{HH}$ = 6.6 Hz
H^3	1.92 (m)	d	$^3J_{HH}$ = 10.4 Hz
$SiCH_2P$	2.47 (dd),	d	$^3J_{HH}$ = 14.3 Hz, $^3J_{PH}$ = 16.3 Hz
$SiCH_2P$	1.91 (t)	d	$^3J_{HH}$ = 15.3 Hz, $^3J_{PH}$ = 15.3 Hz
$SiCH_2P$	1.08 (t),	d	$^3J_{HH}$ = 13.7 Hz, $^3J_{PH}$ = 13.7 Hz
$SiCH_2P$	0.90 (t),	d	$^3J_{HH}$ = 14.0 Hz, $^3J_{PH}$ = 14.0 Hz
SiMe	0.66, 0.65, 0.25, 0.09	s	
Ir-H	-20.42 (t)	s	$^3J_{PH}$ = 11.09 Hz

^{31}P{^{1}H}: 7.20 (d, $^2J_{PP}$ = 4.9 Hz); 9.72 (d, $^2J_{PP}$ = 4.9 Hz).

NOE Experiment

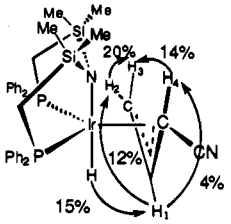

syn-endo
3b

Preparation of Ir(η^3-$CH_2CHCHPh$)H[$N(SiMe_2CH_2PPh_2)_2$] (3c). Styrene (10 equiv) was transferred in a frozen solution of the methylene complex **1** (100 mg, 0.136 mmol) in toluene (20 mL). The solution was allowed to warm up to room temperature and stirred for 18 h to generate a light yellow solution. The solution was pumped to dryness, the residue was redissolved in toluene (0.5 mL), and hexanes were added until the solution became slightly cloudy. Colorless crystals deposited after 3 days. Evaporation of the mother liquor to almost dryness gave a second crop of crystals. The crystals were washed with cold toluene and were dried under vacuum. The combined yield was 78 mg (68%) (Chart 5). Anal. Calcd for $C_{39}H_{46}IrNP_2Si_2$: C, 55.82; H, 5.53; N, 1.67. Found: C, 55.45; H, 5.57; N, 1.55. ^{31}P{^{1}H} NMR (C_6D_6, δ): 7.43 (s), 7.35 (s).

Preparation of Ir(η^3-$CH_2CHCHCOOMe$)H[$N(SiMe_2CH_2PPh_2)_2$] (3d). Methyl acrylate (10 equiv) was transferred into a toluene solution (20 mL) of the methylene complex **1** (100 mg, 0.136 mmol) at −78 °C. When the solution was warmed up to −20 °C, the purple color began to fade, and when the temperature reached 0 °C, a light yellow solution formed. The solution was stirred for 30 min at room temperature and then was pumped to dryness. The residue was recrystallized from hexanes (2 mL) at room temperature to give colorless crystals (Chart 6). Yield: 93 mg (83%). Anal. Calcd for $C_{35}H_{44}IrNO_2P_2Si_2$: C, 51.20; H, 5.40; N, 1.70. Found: C, 51.50; H, 5.60; N, 1.80. ^{31}P{^{1}H} NMR (C_6D_6, δ): 9.62 (s), 7.17 (s).

Preparation of Ir(η^3-$CH_2CHCMeCN$)H[$N(SiMe_2CH_2PPh_2)_2$] (7 and 8). Methacrylonitrile (90 mg, approximately 10 equiv) was vacuum transferred onto a frozen solution of complex **1** in toluene (15 mL). The mixture was warmed up to room temperature and stirred. As soon as the color of the solution turned yellow, the mixture was pumped to dryness. The residue was recrystallized from toluene/hexanes to give a mixture of isomers as a yellow solid. Yield: 76 mg (70%). Anal. Calcd for $C_{35}H_{43}IrN_2P_2Si_2$: C, 52.41; H, 5.40; N, 3.49. Found: C, 52.63; H, 5.70; N, 3.37. ^{31}P{^{1}H} NMR (C_6D_6, δ): major isomer *exo*-**7**, 4.74 (s), 7.09 (s) (Chart 7); minor isomer *endo*-**8**, 6.01 (s), 10.45 (s). The amount of the other two isomers is negligible.

Preparation of Ir(η^3-$CH_2CHCHMe$)H[$N(SiMe_2CH_2PPh_2)_2$] (2e and 3e). To a stirred toluene solution (30 mL) of *mer*-Ir(η^3-CH_2-$CHCHMe$)Br[$N(SiMe_2CH_2PPh_2)_2$] (207 mg, 0.23 mmol) maintained

Chart 5

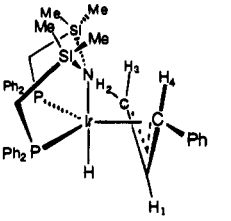

syn-endo
3c

	^{1}H	^{1}H(^{31}P)	J
PPh_2	7.64 - 7.45 (m), 7.45 -7.26 (m)		
	7.24 - 6.87 (m), 6.82 - 6.64 (m)		
	6.8 - 6.7 (m), 6.7 - 6.55 (m)		
	6.64 - 6.41 (m)		
H^1	5.62 (m)	ddd	
H^2	2.56 (m)	d	$^3J_{HH}$ = 6.4 Hz
H^3	2.17(m)	d	$^3J_{HH}$ = 10.5 Hz
H^4	3.91 (t)	d	$^3J_{HH}$ = 9.2 Hz, $^3J_{HP}$ = 9.2 Hz
$SiCH_2P$	2.15 (t)	d	$^3J_{HH}$ = 13.3 Hz, $^3J_{PH}$ = 13.3 Hz
$SiCH_2P$	1.90, 1.88, 1.52(t)	d	$^3J_{HH}$ = 14.0 Hz, $^3J_{PH}$ = 14.0 Hz
SiMe	0.72, 0.66, 0.60, 0.25	s	
Ir-H	-21.67 (t)	s	$^3J_{PH}$ = 11.55 Hz

^{31}P{^{1}H} NMR: 7.43 (s), 7.35 (s).

NOE Experiment

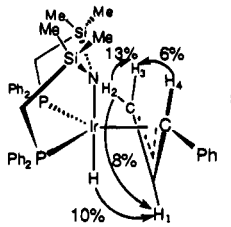

syn-endo
3c

Chart 6

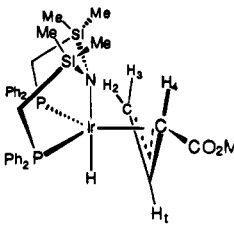

syn-endo
3d

	^{1}H	^{1}H(^{31}P)	J
PPh_2	8.0 - 7.7 (m), 7.4 -7.15 (m)		
	7.15 - 7.05 (m), 7.0 - 6.8 (m)		
	6.8 - 6.7 (m), 6.7 - 6.55 (m)		
	6.55 - 6.45 (m), 6.35 - 6.20(m)		
H^1	6.31 (m)	m	
H^2	2.53 (dd)	d	$^3J_{HH}$ = 6.6 Hz, $^3J_{HP}$ = 9.5 Hz
H^3	2.33 (dd)	d	$^3J_{HH}$ = 11.5 Hz, $^3J_{HP}$ = 16.3 Hz
H^4	3.53 (t)	d	$^3J_{HH}$ = 8.4 Hz, $^3J_{HP}$ = 8.4 Hz
$COO(CH_3)$	2.76 (s)	s	
$SiCH_2P$	2.51 (t),	d	$^3J_{HH}$ = 14.1 Hz, $^3J_{PH}$ = 14.1 Hz
$SiCH_2P$	2.41 (t)	d	$^3J_{HH}$ = 14.0 Hz, $^3J_{PH}$ = 14.0 Hz
$SiCH_2P$	1.83, 1.08 (t),	d	$^3J_{HH}$ = 13.8 Hz, $^3J_{PH}$ = 13.8 Hz
SiMe	0.72, 0.68, 0.52, 0.12	s	
Ir-H	-20.76 (t)	s	$^3J_{PH}$ = 10.65 Hz

NOE Experiment

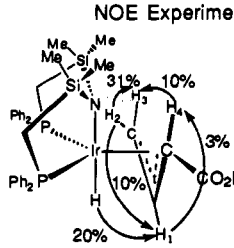

syn-endo
3d

at −78 °C was slowly added $KBEt_3H$ (32 mg, 0.23 mmol) in toluene (20 mL). The mixture was allowed to warm to room temperature, and the solution was stirred overnight to give a light yellow solution. The solution was pumped to dryness to remove the resultant BEt_3. The

Chart 7

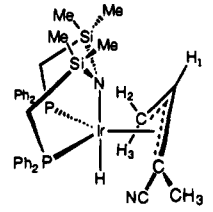

	^{1}H	^{1}H{^{31}P}	J
PPh_2 para	8.0 - 6.5 (m),		
H^1	4.33 (m)	dd	$^3J_{HH}$ = 6.8 Hz, $^3J_{HH}$ = 11.4 Hz
H^2	3.17 (m)	d	$^3J_{HH}$ = 6.8 Hz
H^3	3.52 (m)	d	$^3J_{HH}$ = 11.4 Hz
$SiCH_2P$	2.13, 1.45 (t)	d	$^2J_{HH}$ = $^2J_{PH}$ =14.4 Hz
$SiCH_2P$	1.70 (t)	d	$^2J_{HH}$ = $^2J_{PH}$ =13.9 Hz
$SiCH_2P$	1.27 (t)	d	$^2J_{HH}$ = $^2J_{PH}$ =14.0 Hz
Me	0.87 (d)	s	$^4J_{PH}$ = 3.3 Hz
SiMe	0.57, 0.54, 0.11, 0.07	s	
Ir-H	-20.21 (t)	s	$^3J_{PH}$ = 12.4 Hz

^{31}P{^{1}H} NMR: 7.09 (s), 4.74 (s)

NOE Experiment

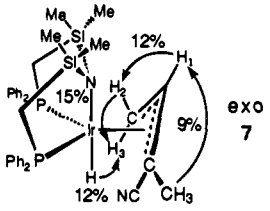

Chart 8

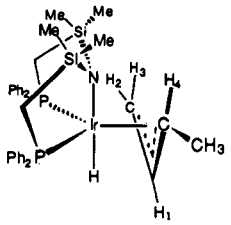

(major isomer)

	^{1}H	^{1}H{^{31}P}	J
PPh_2	7.7 -7.9 (m)		
	7.48 - 7.52 (m)		
	6.8 - 7.4 (m)		
	6.5 - 6.7 (m)		
H^1	4.98 (m)	m	
H^2	2.43 (m)	d	$^3J_{HH}$ = 6.4 Hz
H^3	1.95 (m),	d	$^3J_{HH}$ = 10.2 Hz
H^4	2.77 (m)	m	
$SiCH_2P$	2.28 (t),	d	$^3J_{HH}$ = 14.7 Hz, $^3J_{PH}$ = 14.7 Hz
$SiCH_2P$	1.87, 1.75 (t)	d	$^3J_{HH}$ = 14.0 Hz, $^3J_{PH}$ = 14.0 Hz
$SiCH_2P$	1.40 (t),	d	$^3J_{HH}$ = 13.5 Hz, $^3J_{PH}$ = 13.5 Hz
CH_3	1.22 (dt)	d	$^3J_{HH}$ = 6.1 Hz, $^4J_{PH}$ = 1.6 Hz
SiMe	0.73, 0.71, 0.39, 0.22	s	
Ir-H	-22.15 (t)	s	$^3J_{PH}$ = 11.1 Hz

^{31}P{^{1}H} NMR: 11.3 (s), 7.4 (s).

NOE Experiment

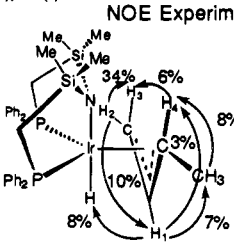

residue was redissolved in toluene and was filtered through Celite. The clear filtrate thus obtained was pumped to dryness again, and the residue was dissolved in hexanes. NMR showed one major isomer and a minor one. Slow evaporation of the solvent at room temperature gave colorless crystals of the major isomer **3e** (Chart 8). Yield: 135 mg (76%). Anal. Calcd for $C_{34}H_{44}NIrP_2Si_2$: C, 52.55; H, 5.70; N, 1.80. Found: C, 52.35; H, 5.74; N, 1.79. ^{31}P{^{1}H} NMR spectrum of the

Chart 9

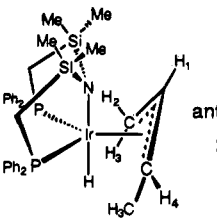

(minor isomer)

	^{1}H	^{1}H{^{31}P}	J
PPh_2 para	8 - 6.5 (m),		
	obscured by the major isomer		
H^1	4.21 (m)	m	
H^2	3.13 (br. d)	d	$^3J_{HH}$ = 7.1 Hz
H^3	2.98 (dd)	d	$^3J_{HH}$ = 11.9 Hz
H^4	4.05 (m)	m	
$SiCH_2P$	obscurred by the major isomer		
SiMe	0.61, 0.59, 0.26, 0.16	s	
Ir-H	-21.47 (t)	s	$^3J_{PH}$ = 13.8 Hz

^{31}P{^{1}H} NMR: 5.7 (s), 4.1 (s)

No NOE experiments were attempted on 2e.

minor isomer **3e** (C_6D_6, δ): 11.3 (s), 7.4 (s). ^{31}P{^{1}H} NMR spectrum of the minor isomer **2e** (C_6D_6, δ): 5.7 (s), 4.1 (s) (Chart 9). No NOE experiments were attempted on **2e**.

X-ray Crystallographic Analyses of Ir(η^3-C_3H_4CN)H[N($SiMe_2CH_2PPh_2$)$_2$]·C_7H_8 (2b·C_7H_8) and Ir(η^3-C_3H_4Me)H[N($SiMe_2CH_2PPh_2$)$_2$] (3e). Crystallographic data appear in Table 1. The final unit-cell parameters were obtained by least-squares on analysis the setting angles for 25 reflections with 2θ = 30.9−35.4° and 32.0−38.6°, respectively, for **2b** and **3e**. The intensities of three standard reflections, measured every 200 reflections throughout the data collections, remained constant for both **2b** and **3e**. The data were processed[26] and corrected for Lorentz and polarization effects and for absorption (empirical, based on azimuthal scans for three reflections).

Both structures were solved by conventional heavy-atom methods. The asymmetric unit of **2b** contains a toluene solvent molecule. The non-hydrogen atoms of both structures were refined with anisotropic thermal parameters. The metal hydride atom of **2b** was placed in a difference map position but could not be refined, and that of **3e** was refined with an isotropic thermal parameter. All other hydrogen atoms were fixed in idealized positions (methyl group orientations staggered or idealized from difference map peaks, C−H = 0.98 Å for **2b** and 0.97 Å for **3e**, $B_H = 1.2B_{\text{bonded atom}}$). Corrections for secondary extinction (Zachariasen type II isotropic) were applied, the final values of the extinction coefficients being 1.57(5) × 10^{-7} for **2b** and 1.01(4) × 10^{-7} for **3e**. Neutral atom scattering factors[27a] and anomalous dispersion corrections[27b] for all atoms were taken from the *International Tables for X-Ray Crystallography*. Final atomic coordinates and equivalent isotropic thermal parameters, complete tables of bond lengths and angles, hydrogen atom parameters, anisotropic thermal parameters, torsion angles, intermolecular contacts, and least-squares planes are included as supplementary material.

Acknowledgment. Financial support for this research was provided by NSERC of Canada. We also thank Johnson Matthey for the generous loan of iridium salts.

Supplementary Material Available: Atomic coordinates and equivalent isotropic thermal parameters, complete tables of bond lengths and bond angles, hydrogen atom parameters, anisotropic thermal parameters, torsion angles, intermolecular contacts, and least-squares planes for **2b** and **3e** (49 pages). Structure factors are available from the authors on request. This material is contained in many libraries on microfiche, immediately follows this article in the microfilm version of the journal, can be ordered from the ACS, and can be downloaded from the Internet; see any current masthead page for ordering information and Internet access instructions.

JA9424641